Estimates of slip weakening distance for different dynamic rupture models

Elisa Tinti, Andrea Bizzarri, Alessio Piatanesi, and Massimo Cocco

Istituto Nazionale di Geofisica e Vulcanologia, Department of Seismology and Tectonophysics, Rome, Italy

[1]   We model the dynamic propagation of a 2-D in-plane crack obeying to either slip weakening (SW) or rate- and state-dependent friction laws (R&S). We compare the value of slip weakening distance (D_c), adopted or estimated from the traction versus slip curves, with the critical slip distance measured as the slip at the time of peak slip velocity (D_c'). The adopted friction law and the constitutive parameters control the slip acceleration as well as the timing and the amplitude of peak slip velocity. Our simulations with R&S show that the direct effect of friction and the friction behavior at high slip rates affect the timing of peak slip velocity and thus control the ratio D_c'/D_c. The difference observed in this study between the D_c values and the inferred D_c' can range between few percent up to 50%.   INDEX TERMS: 3210 Mathematical Geophysics: Modeling; 7209 Seismology: Earthquake dynamics and mechanics; 7215 Seismology: Earthquake parameters; 7260 Seismology: Theory and modeling. **Citation:** Tinti, E., A. Bizzarri, A. Piatanesi, and M. Cocco (2004), Estimates of slip weakening distance for different dynamic rupture models, *Geophys. Res. Lett.*, *31*, L02611, doi:10.1029/2003GL018811.

1.   Introduction

[2]   The determination of temporal evolution of dynamic traction within the cohesive zone during the propagation of an earthquake rupture is the major task of many recent investigations. This evolution is characterized by the traction increase to the upper yield stress (τ_y), which is followed by a decrease to the kinetic friction level (τ_f), during a time interval that defines the duration of the breakdown process. The cohesive zone represents the region of shear stress degradation near the tip of a propagating rupture [*Ida*, 1972; *Andrews*, 1976]. The traction decrease (i.e., the weakening phase) is associated to the slip increase, resulting in the well known slip weakening behavior (Figure 1a). Slip weakening (SW) has been observed in laboratory experiments [*Okubo and Dieterich*, 1984; *Ohnaka et al.*, 1987], it has been proposed in theoretical studies [*Ohnaka*, 2003, and references therein] and used in numerical simulations of earthquake ruptures [*Day*, 1982; *Olsen et al.*, 1997; among many others]. Slip weakening has been demonstrated to occur also with rate and state (R&S) constitutive laws [*Bizzarri and Cocco*, 2003, and references therein].

[3]   Many different approaches have been proposed to estimate the critical slip weakening distance (D_c) for real earthquakes. Most of them rely on the reconstruction of the

traction evolution from kinematic rupture models [*Ide and Takeo*, 1997; *Guatteri and Spudich*, 2000; *Zhang et al.*, 2003]. Recently, *Mikumo et al.* [2003] proposed a method to estimate the critical slip weakening distance from slip velocity functions. The theoretical demonstration of this method is discussed in *Fukuyama et al.* [2003]. This approach is based on the estimate of the slip weakening distance at each point on the fault as the slip (D_c') at the time of peak slip velocity (see Figure 1), supposing that the traction reaches its minimum value in that time. *Fukuyama et al.* [2003] have shown that the estimates of D_c' can be affected by an error of roughly 50%.

[4]   The values of D_c proposed in the recent literature span from microns (laboratory experiments in *Dieterich* [1979]) to several meters [e.g., *Zhang et al.*, 2003]. This raises the question of the actual size of the critical slip weakening distance. In this study we present the results of different numerical simulations of the dynamic propagation of a 2-D in-plane crack obeying different constitutive laws. The goal is to discuss the retrieved slip velocity time histories to verify if the critical slip weakening distance can be estimated from the slip value at the peak slip velocity.

2.   Method

[5]   We solve the elastodynamic equation for a 2-D in-plane crack using a Finite Difference approach [*Andrews*, 1973] and adopting either a SW or a R&S constitutive law with a slowness evolution equation. An extensive presentation of the adopted numerical procedure can be found in *Bizzarri et al.* [2001] and *Bizzarri and Cocco* [2003], who also discuss the required stability and convergence criteria as well as resolution of the cohesive zone. The constitutive laws adopted in this study are given by the following equations:

$$\begin{cases} \tau(V, \Psi) = \tau_* - a\sigma_n^{eff} \ln\left(\dfrac{V_*}{V} + 1\right) + b\sigma_n \ln\left(\dfrac{\Psi V_*}{L} + 1\right) \\ \dfrac{d\Psi}{dt} = 1 - \dfrac{\Psi V}{L} \end{cases} \quad (1)$$

$$\tau = \begin{cases} \tau_y - (\tau_y - \tau_f)\dfrac{u}{D_c}, & u < D_c \\ \tau_f, & u \geq D_c \end{cases} \quad (2)$$

[6]   In Equation (1) (R&S friction law) τ_*, V_* are arbitrary reference values of friction and slip velocity, respectively; a, b and L are the constitutive parameters and σ_n^{eff} is the effective normal stress. Ψ is the state variable
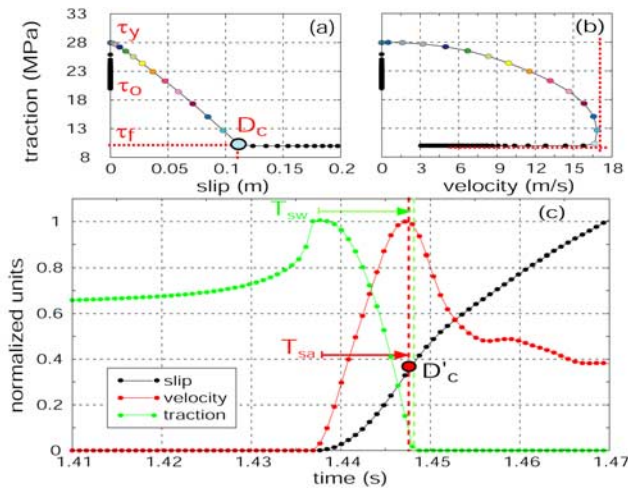
Figure 1. Traction versus slip (a) and slip velocity (b) calculated for a 2-D in-plane crack obeying a SW law for a target point located 5 km from the nucleation. The adopted parameters are listed in Table 1 (Model A). Colors are used to depict the temporal evolution. (c) normalized time histories of total dynamic traction, slip velocity and slip. The dashed lines in (b) emphasize that peak slip velocity is reached when traction is at its minimum value.

that has the meaning of an average contact time between the sliding surfaces. The first logarithmic term in (1) represents the direct effect of friction [*Dieterich*, 1979], while the second accounts for the evolution of the state variable. In Equation (2) (SW law) u is the slip while the other parameters are those defined in Figure 1a.

3. Simulations With a Slip Weakening Law

[7] Figure 1 illustrates the results of a 2-D simulation performed using the SW law (Equation 2) and the input parameters listed in Table 1 (model A). Figure 1a and 1b show the total dynamic traction as a function of slip and slip velocity, respectively, for a target point on the fault; the former depicts the imposed constitutive law, while the latter is part of the solution of the spontaneous dynamic calculation. Figure 1c shows the normalized time history of slip, slip velocity and total dynamic traction. This simulation reveals that the peak of slip velocity occurs exactly when the traction is at its minimum (i.e., the kinetic friction level), consistent with the *Mikumo et al.* [2003] findings. In the present study, we refer to the slip weakening distance inferred from the slip amplitude at the peak slip velocity as D'_c, following *Fukuyama et al.* [2003] and (Spudich and Guatteri, Tests of the accuracy of the D'_c estimate of

earthquake slip-weakening distance, submitted to *Bull. Seism. Soc. Am.*, 2003, hereinafter referred to as Spudich and Guatteri).

[8] As expected, for this simulation D'_c (0.1 m) matches the D_c value assigned as input parameter in the numerical calculation. Because of the low strength value adopted in this simulation ($S = 0.8$, where S is the strength parameter defined by *Das and Aki* [1977]), the rupture speed becomes super-shear and the resulting peak slip velocity is very high. The time coincidence between the peak of slip velocity and the minimum traction implies that the temporal duration of slip weakening phase (T_{sw}) is equal to the duration of slip acceleration phase (T_{sa}), as shown in Figure 1. In other words, the slip acceleration during the weakening phase is always positive. Because this should rely on the fault constitutive properties, in this paper we investigate whether this behavior is common in constitutive formulations other than SW, widely adopted in the literature.
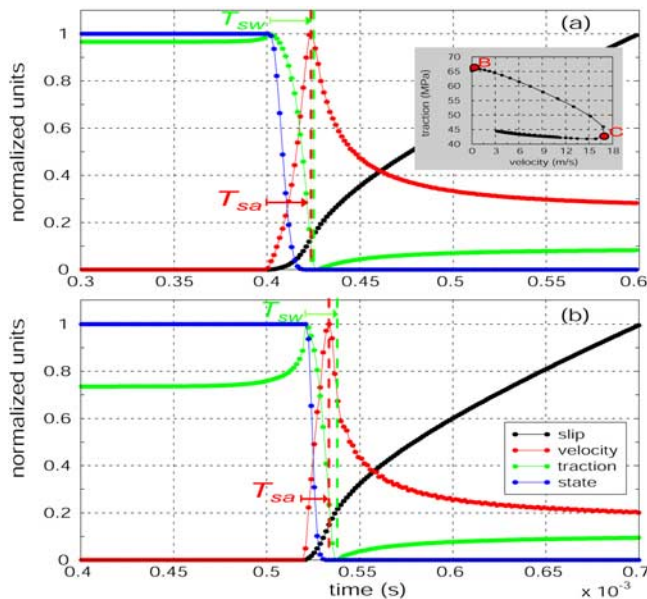
4. Simulations With Rate and State Laws

[9] We present the results of several simulations performed to model the spontaneous dynamic propagation of a 2-D in-plane crack obeying to the R&S law (Equation 1). Figure 2a shows the normalized time histories of slip, slip velocity, traction and state variable calculated with the parameters listed in Table 1 (Model B). This set of parameters is based on laboratory experiments results. For this simulation D_c inferred from the traction versus slip curve is 0.16 mm. This figure clearly points out that the peak of slip velocity occurs well before that the traction reaches the
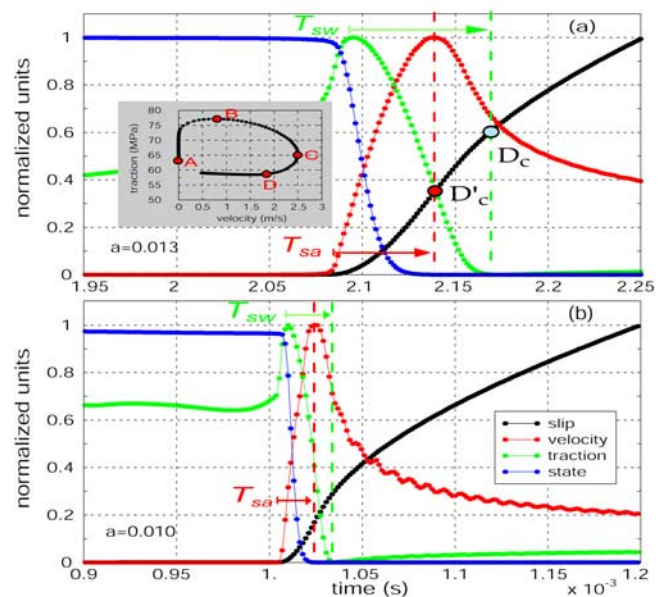
Figure 2. Normalized time histories of different physical quantities computed for a 2-D in-plane crack obeying R&S friction. The inset in panel (a) displays the traction as a function of slip velocity (phase diagram). The used constitutive parameters are listed in Table 1 (Model B). (b) same as above with a smaller value of a parameter (0.010). Capital letters identify the different stage of the breakdown process.

Table 1. Medium and Constitutive Parameters

Model A - SW		Model C - SW
[S = 0.8]	*Model B - R&S*	[S = 1.5]
σ_n^{eff} = 30 MPa	σ_n^{eff} = 100 MPa	σ_n^{eff} = 30 MPa
τ_0 = 20 MPa	a = 0.013	τ_0 = 20 MPa
τ_y = 28 MPa	b = 0.017	τ_y = 24.5 MPa
τ_f = 10 MPa	$L = 10^{-5}$ M	τ_f = 17.7 MPa
D_c = 0.1 m	Ψ_{init} = 1s; $V_{init} = 10^{-5}$ m/s	D_c = 0.1 m

ρ = 2700 Kg/m³; α = 3000 m/s; β = 5196 m/s.

Figure 3. Normalized time histories of physical quantities computed with model B of Table 1 and a slip velocity cutoff (V_{cut}) on friction at high slip rates. In Panel (a) V_{cut} is $2 \cdot 10^{-5}$ m/s, slightly larger than the initial velocity ($1 \cdot 10^{-5}$ m/s), while in panel (b) V_{cut} is $2 \cdot 10^{-3}$ m/s. The inset in panel (a) shows the associated phase diagram.

kinematic stress level. This is also evident looking at the phase diagram displayed in the inset of Figure 2a, that shows a stage in which both slip velocity and traction decrease (C-D in Figure 2a). In this case, the value of D'_c is 0.085 mm, roughly 50% of D_c. Because we are interested here only to relative differences between D_c and D'_c, we do not face the problem of scaling the laboratory values to real fault dimensions. The friction law controls the evolution of slip velocity and the timing of its peak. Therefore, in the framework of R&S friction, it is the state variable evolution that controls the weakening phase and the slip acceleration [see *Cocco and Bizzarri*, 2002].

4.1. The Direct Effect of Friction

[10] We have performed many different simulations by changing the constitutive parameters. We discuss here the effect of changing the parameter a controlling the direct effect of friction in Equation (1). Figure 2b shows the time histories of the relevant physical quantities calculated for the same set of parameters used in Figure 2a, but using a smaller value of the a parameter (0.010). In this case the timing of peak slip velocity is still not coincident with the time at which the traction reaches the kinetic level, but their difference is smaller than that shown in Figure 2a. In this simulation D_c is 0.18 mm, while D'_c is 0.12 mm. Our numerical results suggest that the direct effect of friction controls the occurrence and the amplitude of slip velocity peaks. However, we have to remark that, by reducing the parameter a, we change both the yield and the kinetic stress values as discussed by *Bizzarri and Cocco* [2003].

### 4.2. Friction Behavior at High Slip Rates

[11] The previous results motivated a further test. We have performed several simulations modifying the friction

behavior at high slip rates defined by Equation (1). We have assumed that, when the slip velocity exceeds a fixed threshold (V_{cut}), the direct friction term [$\ln(V_*/V)$] in Equation (1) is frozen and taken constant [$\ln(V_*/V_{cut})$] [*Weeks*, 1993]. This implies that for $V > V_{cut}$ the governing Equation (1) does not directly depend on slip velocity, although the dependence on slip rate is still present in the state variable evolution. We show in Figure 3 the results of two simulations performed by using the parameters listed in Table 1 (Model B), with $a = 0.012$ and two different values of V_{cut}. In panel (a) the slip velocity cutoff is slightly larger than the initial velocity ($V_{cut} = 2\ V_{init}$); therefore, the direct effect of friction is constant for most of the simulation. On the contrary, in panel (b) V_{cut} is two orders of magnitude larger (200 V_{init}). Our simulations point out that the peak of slip velocity and the minimum traction are reached at similar times if the direct effect of friction is taken constant; this is also evident looking at the phase diagram displayed in the inset of panel (a). The critical slip distances inferred from the simulation shown in Figure 3a are $D_c = 0.23$ mm and $D'_c = 0.18$ mm.

5. Discussion and Concluding Remarks

[12] The simulations discussed above demonstrate that using R&S dependent laws, the slip velocity evolution is controlled by the adopted friction law, its behavior at high slip rates and the constitutive parameters. We will show here that also using a SW law the timing of peak slip velocity depends on the assumed constitutive parameters. The simulation shown in Figure 1 is representative of a relatively low-strength fault ($S = 0.8$). For the homogeneous configuration here considered, this implies that during propagation, the rupture accelerates to super-shear speeds. We show in Figure 4 another simulation performed using a SW law with a higher strength parameter ($S = 1.5$). The model parameters are listed in Table 1 (Model C). In this case the rupture velocity is sub-shear. Figure 4 displays the time evolution of the normalized physical quantities and points out that peak of slip velocity occurs before the traction reaches its minimum. The inferred difference between D_c and D'_c is slightly less than 30%.

[13] Our simulations demonstrate that the phase diagrams reflect the differences between D_c and D'_c. In particular, when the peak of slip velocity is simultaneous with the minimum traction, the phase diagram consists of an extremely fast slip acceleration. This is evident com-
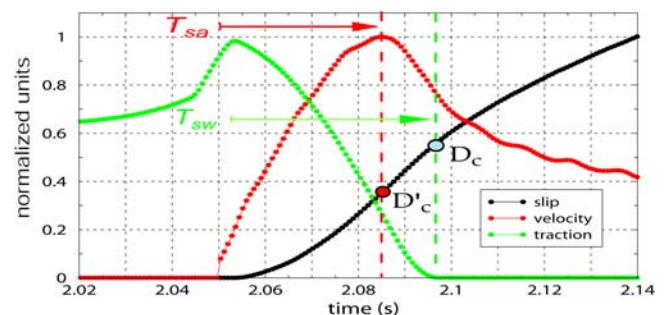
Figure 4. Normalized time histories of physical quantities for a calculation performed with a SW law and the model parameters listed in Table 1 (Model C). The strength value (1.5) is larger than that of Figure 1 (0.8).

paring Figure 1b and the inset in Figure 3a with the phase diagram shown in Figure 2a. *Fukuyama and Madariaga* [1998] proposed the following boundary condition relating traction $[\tau]$ to slip velocity $[V]$ and slip $[u]$ on the fault plane:

$$\tau(x,t) = -\frac{\mu}{2\beta}V(x,t) + \int_S \int_0^t K\left(x - \vec{\xi}; t - t'\right) u\left(\vec{\xi}, t'\right) dt' dS \quad (3)$$

where μ and β are the rigidity and the shear wave velocity, respectively. K is the integration kernel, which accounts for the contribution of the past slip history. This relation is independent of the constitutive law, although friction controls the slip and slip velocity functions included in (3). Equation (3) is useful to interpret our results and the different phase diagrams obtained in this study. The phase diagrams shown in Figures 1 and 3 are characterized by large values of slip velocity and, as a consequence, by large values of dynamic load due to previous slip history [i.e., the integral term in (3)]. In these conditions, we found that $D_c \sim D_c'$. We have to emphasize however that these simulations yield unrealistic values of slip velocity. On the contrary, the shape of the phase diagram shown in Figure 2a is characterized by smaller contributions of the dynamic load and a reduced slip acceleration. In this case, we found that D_c' is 50% of D_c.

[14] The results obtained in this study generalize the *Fukuyama et al.* [2003] conclusions. We show that the variability of fault constitutive properties can explain the observed differences between D_c' and D_c. Spudich and Guatteri tested the accuracy of D_c' estimates and found that low pass filtering of slip models can bias the inferred values causing an artificial correlation between D_c' and total slip. In our calculations the peak slip velocity always occurs within the breakdown time and then D_c' is smaller than D_c.

[15] We can therefore conclude that the estimated value of the parameter D_c' is affected by the friction law and the constitutive parameters, which control the slip acceleration and the traction drop during the breakdown time. The differences found in this study between D_c' and D_c can vary from few percent up to 50%, in agreement with *Fukuyama et al.* [2003]. These results are consistent with the simulations presented in *Perrin et al.* [1995], (see Figure 2 of that paper). Although the biases pointed out by *Guatteri and Spudich* [2000] and Spudich and Guatteri might represent a limitation to constrain the actual critical slip weakening distance, the estimate of D_c' might be still useful if we accept the idea that D_c can range over several order of magnitudes. In this case an error of 50% in D_c', can still allow us to constrain the size of the critical slip weakening distance.

References

Andrews, D. J. (1973), A numerical study of tectonic stress release by underground explosions, *Bull. Seismol. Soc. Am.*, *63*, 1375–1391.

Andrews, D. J. (1976), Rupture velocity of plane strain shear crack, *J. Geophys. Res.*, *81*, 5679–5687.

Bizzarri, A., and M. Cocco (2003), Slip-weakening behavior during the propagation of dynamic ruptures obeying rate- and state-dependent friction laws, *J. Geophys. Res.*, *108*(B8), 2373, doi:10/1029/2002JB002198.

Bizzarri, A., M. Cocco, D. J. Andrews, and E. Boschi (2001), Solving the dynamic rupture problem with different approaches and constitutive laws, *Geophys. J. Int.*, *144*, 656–678.

Cocco, M., and A. Bizzarri (2002), On the slip-weakening behavior of rate- and state dependent constitutive laws, *Geophys. Res. Lett.*, *29*(11), 1516, doi:10.1029/2001GL013999.

Das, S., and K. Aki (1977), A numerical study of two-dimensional spontaneous rupture propagation, *Geophys. J. R. Astron. Soc.*, *50*, 643–668.

Day, S. M. (1982), Three-dimensional finite difference simulation of fault dynamics: Rectangular faults with fixed rupture velocity, *Bull. Seismol. Soc. Am.*, *72*, 705–727.

Dieterich, J. H. (1979), Modeling of rock friction - 1. Experimental results and constitutive equations, *J. Geophys. Res.*, *84*, 2161–2168.

Fukuyama, E., and R. Madariaga (1998), Rupture dynamics of a planar fault in a 3-D elastic medium: Rate- and slip-weakening friction, *Bull. Seismol. Soc. Am.*, *88*, 1–17.

Fukuyama, E., T. Mikumo, and K. B. Olsen (2003), Estimation of the critical slip-weakening distance: Theoretical background, *Bull. Seismol. Soc. Am.*, *93*, 1835–1840.

Guatteri, M., and P. Spudich (2000), What can strong-motion data tell us about slip-weakening fault-friction laws?, *Bull. Seismol. Soc. Am.*, *90*(1), 98–116.

Ida, Y. (1972), Cohesive force across the tip of a longitudinal-shear crack and Griffith's specific surface energy, *J. Geophys. Res.*, *77*, 3796–3805.

Ide, S., and M. Takeo (1997), Determination of constitutive relations of fault slip based on seismic wave analysis, *J. Geophys. Res.*, *102*(B12), 27,379–27,392.

Mikumo, T., K. B. Olsen, E. Fukuyama, and Y. Yagi (2003), Stress-breakdown time and slip-weakening distance inferred from slip-velocity functions on earthquake faults, *Bull. Seismol. Soc. Am.*, *93*, 264–282.

Ohnaka, M. (2003), A constitutive scaling law and a unified comprehension for frictional slip failure, shear fracture of intact rock, and earthquake rupture, *J. Geophys. Res.*, *108*(B2), 2080, doi:10.1029/2002JB00123.

Ohnaka, M., Y. Kuwahara, and K. Yamamoto (1987), Constitutive relations between dynamic physical parameters near a tip of the propagation slip zone during stick-slip shear failure, *Tectonophysics*, *144*, 109–125.

Okubo, P. G., and J. H. Dieterich (1984), Effects of physical fault properties on frictional instabilities produced on simulated faults, *J. Geophys. Res.*, *89*, 5817–5827.

Olsen, K. B., R. Madariaga, and R. J. Archuleta (1997), Three-dimensional dynamic simulation of the 1992 Landers earthquake, *Science*, *278*, 834–838.

Perrin, G., J. R. Rice, and G. Zheng (1995), Self-healing slip pulse on a frictional surface, *J. Mech. Phys. Solids*, *43*, 1461–1495.

Weeks, J. (1993), Constitutive laws for high-velocity frictional sliding and their influence on stress drop during unstable slip, *J. Geophys. Res.*, *98*(B10), 17,637–17,648.

Zhang, W., T. Iwata, K. Irikura, H. Sekiguchi, and M. Bouchon (2003), Heterogeneous distribution of the dynamic source parameters of the 1999 Chi-Chi, Taiwan, earthquake, *J. Geophys. Res.*, *108*(B5), 2232, doi:10.1029/2002JB001889.

———————————

E. Tinti, A. Bizzarri, A. Piatanesi, and M. Cocco, Istituto Nazionale di Geofisica e Vulcanologia, Via di Vigna Murata, 605, 00143 Rome, Italy. (tinti@ingv.it; bizzarri@bo.ingv.it; piatanesi@ingv.it; cocco@ingv.it)